for the MSSW as v_0 becomes greater than v_p. The energy from the semiconductor is received—wholly ($Q_3 = 0$) or partly ($Q_3 < |Q_2|$)—by the MSSW and, consequently, the amplitude of the waves becomes larger. But if YIG damping is so great that $Q_3 > |Q_2|$, the radiated energy is all dissipated in YIG loss and does not contribute to the amplification.

IV. Conclusion

In the preceding section, the amplifying characteristics of the MSSW WW mode caused by a carrier flow in semiconductor have been investigated by using the dispersion equation and the energy conservation law for almost transparent media. It is pointed out that the WW mode is favorable to amplification, since it has a backward branch interacting with a slower drifting carrier. One of the important results of our energy analysis is that the MSSW instability occurs only when the energy dissipation of the media is negative for the waves. If this result is combined with Schlömann's microscopic and qualitative work [15], one may easily appreciate the amplifying mechanism of this type physically and construct a total picture of the system.

References

[1] N. S. Chang and Y. Matsuo, "Possibility of utilizing the coupling between a backward wave in YIG and waves associated with drift carrier stream in semiconductor," *Proc. IEEE*, vol. 56, pp. 765–766, Apr. 1968.
[2] A. V. Vashkovskii, V. I. Zubkov, V. N. Kildshev, and B. A. Murmuzhev, "Interaction of surface magnetostatic waves with carrier on a ferrite-semiconductor interface," *Sov. Phys. JETP Letters*, vol. 16, pp. 4–7, 1972.
[3] M. Szustakowski and B. Wecki, "Amplification of a magnetostatic surface wave in the YIG-Ge hybrid system," *Proc. of Vibration Problems*, vol. 14, pp. 155–163, 1973.
[4] V. P. Lukomskii and Yu. A. Tsvirko, "Amplification of magnetostatic waves in a ferromagnetic film due to the drift current of carriers," *Sov. Phys. Solid State*, vol. 15, pp. 492–495, 1973.
[5] M. Masuda, N. S. Chang, and Y. Matsuo, "Magnetostatic surface waves in ferrite slabs adjacent to semiconductor," *IEEE Trans. Microwave Theory Tech.*, vol. MTT-22, pp. 132–135, Feb. 1974.
[6] N. S. Chang, S. Yamada, and Y. Matsuo, "Characteristics of magnetostatic surface-wave propagation in a layered structure consisting of metals, dielectrics, a semiconductor and Y.I.G.," *Electron. Lett.*, vol. 11, pp. 83–85, Feb. 1975.
[7] ——, "Amplification of magnetostatic surface waves in a layered structure consisting of metals, dielectrics, a semiconductor and Y.I.G.," *J. Appl. Phys.*, vol. 47, pp. 385–387, Jan. 1976.
[8] R. E. De Wames and T. J. Wolfram, "Characteristics of magnetostatic surface waves for a metalized ferrite slab," *J. Appl. Phys.*, vol. 41, pp. 5243–5246, Dec. 1970.
[9] H. Van De Vraat, "Influence of metal plate on surface magnetostatic modes of magnet slab," *Electron. Lett.*, vol. 6, pp. 601–602, Sept. 1970.
[10] T. Musha, "Wave amplification in moving dispersive media," *IECE Japan*, vol. 51, pp. 614–620 (Part I), May 1968, pp. 760–765 (Part II), June 1968.
[11] T. Musha and M. Agu, "Energy and power flow of a moving dispersive media," *J. Phys. Soc. Japan*, vol. 26, pp. 541–549, Feb. 1969.
[12] S. R. Seshadri, "Surface magnetostatic modes of a ferrite slab," *Proc. IEEE*, vol. 58, pp. 506–507, Mar. 1970.
[13] R. W. Damon and J. R. Eshbach, "Magnetostatic modes of a ferromagnet slab," *J. Phys. Chem. Solid*, vol. 118, pp. 308–320, July 1960.
[14] R. J. Briggs, *Electron Stream Interaction with Plasma*. MIT Press, 1964.
[15] E. Schlömann, "Amplification of magnetostatic surface waves by interaction with drifting charge carriers in crossed electric and magnetic fields," *J. Appl. Phys.*, vol. 40, pp. 1422–1424. Mar. 1969.

On Microwave-Induced Hearing Sensation

JAMES C. LIN, MEMBER, IEEE

***Abstract*—When a human subject is exposed to pulsed microwave radiation, an audible sound occurs which appears to originate from within or immediately behind the head. Laboratory studies have also indicated that evoked auditory activities may be recorded from cats, chinchillas, and guinea pigs. Using a spherical model of the head, this paper analyzes a process by which microwave energy may cause the observed effect. The problem is formulated in terms of thermoelasticity theory in which the absorbed microwave energy represents the volume heat source which depends on both space and time. The inhomogeneous thermoelastic motion equation is solved for the acoustic wave parameters under stress-free surface conditions using boundary value technique and Duhamel's theorem. Numerical results show that the predicted frequencies of vibration and threshold pressure amplitude agree reasonably well with experimental findings.**

Manuscript received July 12, 1976; revised October 5, 1976. This work was supported in part by the National Science Foundation under Grant ENG 75-15227.

The author is with the Department of Electrical and Computer Engineering, Wayne State University, Detroit, MI 48202.

I. Introduction

IT HAS BEEN demonstrated that sound can be generated in laboratory animals by the absorption of microwave energy in the head [1]–[3]. These reports indicate that auditory activities may be evoked by irradiating the heads of cats, chinchillas, and guinea pigs with pulsed microwave energy [1], [4]–[6]. Responses elicited in cats by both conventional acoustic stimuli and by pulsed microwaves disappear following destruction of the round window of the cochlea [4], and following death [3]. This suggests that microwave-induced audition is transduced by a mechanism similar to that responsible for conventional acoustic reception, and that the primary site of interaction resides peripherally with respect to the cochlea. More recently [6], sonic oscillations at 50 kHz have been recorded from the round window of guinea pigs during irradiation by pulsed

TABLE I
ELASTIC AND THERMAL PROPERTIES OF BRAIN MATTER

Specific heat, c_h	0.88 cal/gm-°C
density, ρ	1.05 gm/cm^3
coefficient of thermal expansion, α	4.1 x 10^{-5}/°C
Lame's constant, λ	2.24 x 10^{10}dyn/cm^2
Lame's constant, μ	10.52 x 10^3dyn/cm^2
Bulk velocity of propagation, c_1	1.460 x 10^5cm/sec

microwaves at 918 MHz. The oscillations promptly followed onset of radiation, preceded the nerve responses, and disappeared after death. It is therefore reasonable to conclude that the microwave-induced auditory effect is a cochlear response to acoustic signals that are generated, presumably in the head, by pulsed microwaves.

When human subjects are exposed to pulsed microwave radiation, an audible sound occurs which appears to originate from within or immediately behind the head. The microwave-generated sound has been described as clicking, buzzing, or chirping depending on such factors as pulsewidth and repetition rate [2], [4], [5], [7], [8]. The effect is of great significance since the average incident power densities required to elicit the response are considerably lower than those found for other microwave biological effects and the threshold average power densities are many orders of magnitude smaller than the current safety standard of 10 mW/cm^2 [9].

Although the effect is widely accepted as a genuine biologic effect occurring at low average power densities, there exists some controversy regarding the mechanism by which pulsed microwave energy is converted to sound [1], [4], [7], [10]–[13]. This paper analyzes the acoustic wave generated in the heads of animals and man exposed to pulsed microwave radiation as a result of rapid thermal expansion.

We assume that the auditory effect arises from the minuscule but rapid rise of temperature in the brain as a result of absorption of microwave energy. The rise of temperature occurring in a very short time is believed to create thermal expansion of the brain matter which then launches the acoustic wave of pressure that is detected by the cochlea [13].

We consider the head to be perfectly spherical and consisting only of brain matter. The impinging radiation is assumed to be a plane wave of pulsed microwave energy. Our approach is first to obtain the absorbed microwave energy inside the head. The accompanying temperature rise is then derived, and finally the inhomogeneous thermoelastic motion equation is solved for the acoustic wave generated in the head.

The relevant physical parameters of brain matter are listed in Table I. All except one are typical values obtained from the literature [14]–[16]. For the coefficient of thermal expansion, which does not seem to have been measured in the past, we assume a value equal to 60 percent of the corresponding value for water. These values will be useful for quantitative estimations of the frequency and threshold of pulsed microwave-induced hearing.

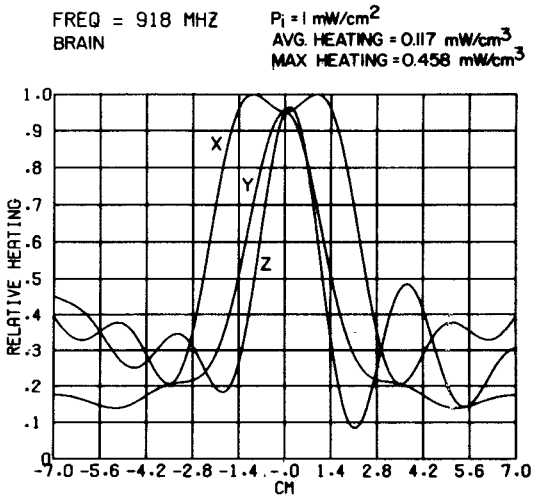

Fig. 1. Absorbed energy distribution in a 7-cm-radius spherical model of the head exposed to 918-MHz plane wave. The incident power density is 1 mW/cm^2 [20].

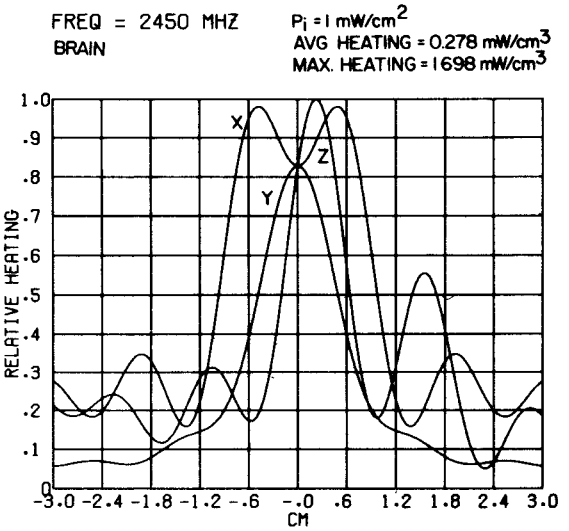

Fig. 2. Absorbed energy distribution in a 3-cm-radius spherical model of the head exposed to 2450-MHz plane wave. The incident power density is 1 mW/cm^2 [20].

II. THEORETICAL FORMULATION

A. Microwave Absorption

Let us consider a homogeneous spherical model of the head exposed to a plane wave of pulsed microwave energy. The absorbed microwave energy $I(r,t)$ at any point inside the head is given by

$$I(r,t) = \tfrac{1}{2}\sigma|\bar{E}|^2 \tag{1}$$

where σ is the electrical conductivity of brain matter. The induced electric field $\bar{E}$ is given by

$$\bar{E} = E_0 e^{-i\omega t} \sum_{j=1}^{\infty} i^j \frac{2j+1}{j(j+1)} [a_j \bar{M}_{01j} - ib_j \bar{N}_{e1j}] \tag{2}$$

where E_0 is the incident electric field strength, $\omega = 2\pi f$, f is frequency, a_j and b_j are magnetic and electric oscilla-

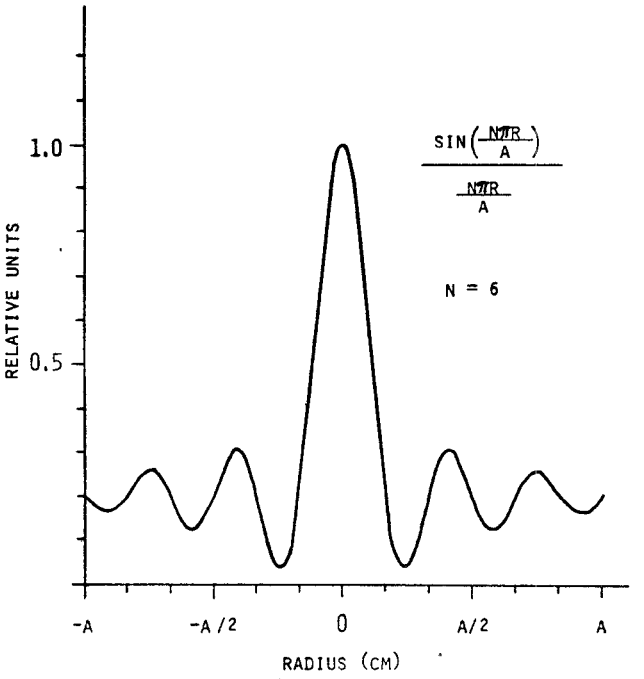

Fig. 3. The approximated absorbed energy distribution.

tions, respectively, and $\overline{M}$ and $\overline{N}$ are vector spherical wave functions. A derivation of (2) may be found in [17]. The detailed expressions are also given in [18].

For humans exposed to 918-MHz radiations and small animals such as cats exposed to 2450 MHz, the absorbed energy distributions inside the head computed from (1) and (2) show absorption peaks in the center of the head [19], [20]. Plots of the absorbed energy distribution along the three rectangular coordinate axes of a 7.0-cm-radius spherical head exposed to 918 MHz and a 3.0-cm-radius spherical head exposed to 2450-MHz plane waves are shown in Figs. 1 and 2. The plane wave impinges from the negative z direction and is polarized in the x direction. Note that in both cases the absorbed energy along the three coordinate axes exhibits characteristic oscillations along the outer portion of the spherical head and reaches a maximum near the center.

Although the detailed absorption along the three axes is not the same, we will assume a spherically symmetric absorption pattern and approximate the absorbed energy distribution inside the head by the spherically symmetric function

$$W(r,t) = I_0 \sin\left(\frac{N\pi r}{a}\right) \Big/ \left(\frac{N\pi r}{a}\right) \tag{3}$$

where I_0 is the peak absorbed energy per unit volume, r is the radial variable, and a is the radius of the spherical head. The parameter N specifies the number of oscillations in the approximated spatial dependence of the absorbed energy. Fig. 3 shows the approximated energy absorption pattern for $N = 6$ and is particularly suited for the cases shown in Figs. 1 and 2. For some frequencies and sphere sizes, the integer N may be changed to account for the difference in absorption patterns. For instance, $N = 3$ may be chosen to approximate the absorption pattern inside a 5-cm-radius spherical head exposed to 918-MHz radiation [20]. For other frequencies and sphere sizes, a different function will be required to describe the absorbed energy distribution.

B. Temperature Rise

We take advantage of the symmetry of the absorbed energy pattern by expressing the heat conduction equation as a function of r alone [21]. That is,

$$\frac{1}{r^2}\frac{\partial}{\partial r} r^2 \frac{\partial v}{\partial r} - \frac{1}{\kappa}\frac{\partial v}{\partial t} = \frac{-W(r,t)}{K} \tag{4}$$

where v is temperature, κ and K are, respectively, the thermal diffusivity and conductivity of brain matter, and W is the heat production rate, which is the same as the absorbed microwave energy pattern and is assumed for the moment to be constant over time.

Because microwave absorption occurs in a very short time interval, there will be little chance for heat conduction to take place. We may therefore neglect the spatial derivatives in (4) such that

$$\frac{1}{\kappa}\frac{dv}{dt} = \frac{W}{K}. \tag{5}$$

Equation (5) may be integrated, directly, to give the change in temperature by setting the initial temperatures equal to zero. Thus

$$v(r,t) = \frac{I_0}{\rho c_h} \frac{\sin(N\pi r/a)}{N\pi r/a}\, t \tag{6}$$

where ρ and c_h are the density and specific heat of brain matter, respectively, and $\rho c_h = K/\kappa$.

In biological materials, the stress-wave development times are short compared with temperature equilibrium times. The temperature decay is therefore a slowly varying function of time and becomes significant only for times greater than milliseconds. We may thus assume for a square pulse of microwave energy, immediately after termination of radiation, that

$$v(r,t) = \frac{I_0}{\rho c_h} \frac{\sin(N\pi r/a)}{N\pi r/a}\, t_0 \tag{7}$$

where t_0 is the pulsewidth.

C. Sound Generation

We now consider the spherical head with homogeneous brain matter as a linear, elastic medium without viscous damping. The thermoelastic equation of motion in spherical coordinates [22] is then given by

$$\frac{\partial^2 u}{\partial r^2} + \frac{2}{r}\frac{\partial u}{\partial r} - \frac{2}{r^2}u - \frac{1}{c_1^2}\frac{\partial^2 u}{\partial t^2} = \frac{\beta}{\lambda + 2\mu}\frac{\partial v}{\partial r} \tag{8}$$

where u is the displacement of brain matter, $c_1 = [(\lambda + 2\mu)/\rho]^{1/2}$ is the velocity of bulk acoustic wave propagation, $\beta = \alpha(3\lambda + 2\mu)$, α is the coefficient of linear thermal expansion, and λ and μ are Lame's constants. It should be noted that the curl of u equals zero since u is in the radial

direction only. The right-hand side of (8) is the change in temperature which gives rise to the displacement. We first write

$$\frac{\beta}{\lambda + 2\mu} \frac{\partial v}{\partial r} = u_0 F_r(r) F_t(t). \tag{9}$$

Hence

$$u_0 = \frac{I_0}{\rho c_h} \frac{\beta}{\lambda + 2\mu} \tag{10}$$

and

$$F_r(r) = \frac{d}{dr}\left[\sin\left(\frac{N\pi r}{a}\right) \Big/ \left(\frac{N\pi r}{a}\right)\right]. \tag{11}$$

From (6) and (7), we have

$$F_t(t) = \begin{cases} t, & 0 \le t \le t_0 \\ t_0, & t \ge t_0. \end{cases} \tag{12}$$

If the surface of the sphere is stress free, then the boundary condition at $r = a$ is

$$(\lambda + 2\mu) \frac{\partial u}{\partial r} + 2\lambda \frac{u}{r} = \beta v = 0. \tag{13}$$

The initial conditions are

$$u(r,0) = \frac{\partial u(r,0)}{\partial t} = 0. \tag{14}$$

Our approach in the following derivations is first to obtain a solution for the case of step of microwave energy, $F_t(t) = 1$, at some instant $t = 0$ and then to extend the solution to a rectangular pulse using Duhamel's theorem [23].

1) Unit Step: If we write the displacement $u(r,t)$ as

$$u(r,t) = u_s(r) + u_t(r,t) \tag{15}$$

and substitute (15) into (8), the equation of motion becomes two differential equations: a stationary one and a time-varying one. Thus

$$\frac{d^2 u_s(r)}{dr^2} + \frac{2}{r}\frac{du_s(r)}{dr} - \frac{2}{r^2} u_s(r) = u_0 F_r(r) \tag{16}$$

and

$$\frac{\partial^2 u_t(r,t)}{\partial r^2} + \frac{2}{r}\frac{\partial u_t(r,t)}{\partial r} - \frac{2}{r^2} u_t(r,t) = \frac{1}{c_1^2}\frac{\partial^2 u_t(r,t)}{\partial t^2}. \tag{17}$$

The corresponding boundary conditions at $r = a$ are

$$(\lambda + 2\mu)\, du_s/dr + 2\lambda u_s/r = 0 \tag{18}$$

and

$$(\lambda + 2\mu)\, \partial u_t/\partial r + 2\lambda u_t/r = 0. \tag{19}$$

To obtain $u_s(r)$, we assume a solution of the form

$$u_s(r) = u_p(r) + D_1/r^2 + D_2 r \tag{20}$$

where $u_p(r)$ is a particular solution of (16). We now rewrite the left-hand side of (16) as follows:

$$\frac{d}{dr}\left[\frac{1}{r^2}\frac{d(r^2 u_p)}{dr}\right] = u_0 F_r(r). \tag{21}$$

We then integrate (21) from 0 to r to get the expression

$$u_p(r) = u_0\left(\frac{a}{N\pi}\right) j_1\left(\frac{N\pi r}{a}\right). \tag{22}$$

Since $u_s(r)$ must remain finite as $r \to 0$, D_1 reduces immediately to zero. The coefficient D_2 is obtained by applying the boundary condition of (18), and it is

$$D_2 = \pm u_0 \left(\frac{1}{N^2\pi^2}\right) \frac{4\mu}{3\lambda + 2\mu}, \qquad N = \begin{cases} 1,3,5\cdots \\ 2,4,6\cdots \end{cases}. \tag{23}$$

The solution of (16) is therefore given by

$$u_s(r) = u_0 \left[\frac{a}{N\pi} j_1\left(\frac{N\pi r}{a}\right) \pm \frac{4\mu}{3\lambda + 2\mu}\frac{r}{N^2\pi^2}\right], \qquad N = \begin{cases} 1,3,5\cdots \\ 2,4,6\cdots \end{cases} \tag{24}$$

where $j_1(N\pi r/a)$ is the spherical Bessel function of the first kind and first order.

Now we let

$$u_t(r,t) = R(r)T(t) \tag{25}$$

and use the method of separation of variables to solve (17) for the time-varying component. Inserting (25) into (17) yields the two ordinary differential equations

$$\frac{d^2 R}{dr^2} + \frac{2}{r}\frac{dR}{dr} + \left(k^2 - \frac{2}{r^2}\right) R = 0 \tag{26}$$

$$\frac{d^2 T}{dt^2} + k^2 c_1^2 T = 0 \tag{27}$$

where k is the constant of separation to be determined. Equation (26) is Bessel's equation and its solution is [17]

$$R(r) = B_1 j_1(kr) + B_2 y_1(kr) \tag{28}$$

where $j_1(kr)$ and $y_1(kr)$ are the spherical Bessel functions of the first and second kind of the first order. Since $R(r)$ is finite at $r = 0$, B_2 must be zero. Combining (28) and the boundary condition of (19), we obtain a transcendental equation for k, the constant of separation,

$$\tan(ka) = (ka)/[1 - (\lambda + 2\mu)(ka)^2/(4\mu)]. \tag{29}$$

The solution of (29) is an infinite sequence of eigenvalues k_m; each corresponds to a characteristic mode of vibration of the spherical head. It can be shown that, using the values for brain matter given in Table I, $k_m a = m\pi$, $m = 1,2,3\cdots$ to within an accuracy of 10^{-7}. Moreover, since (27) is harmonic in time, a general solution for $u_t(r,t)$ may be written as

$$u_t(r,t) = \sum_{m=1}^{\infty} A_m j_1(k_m r) \cos \omega_m t \tag{30}$$

where

$$\omega_m = k_m c_1 = m\pi c_1/a \tag{31}$$

and ω_m is the angular frequency of vibration of the sphere. Note that the frequency of vibration is independent of the absorbed energy pattern. It is only a function of the spherical head size and the elastic properties of the medium.

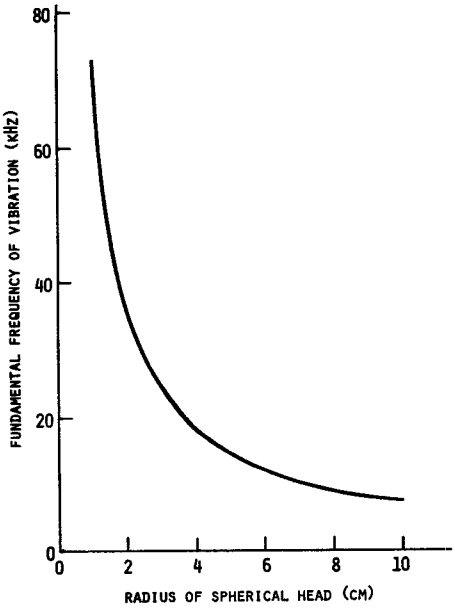

Fig. 4. The fundamental frequencies of sound generated inside the head as a function of spherical head radii.

The fundamental frequency of sound generated inside the spherical head is therefore given by

$$f_1 = c_1/2a. \tag{32}$$

Fig. 4 is a plot of the fundamental frequency of sound generated in the head as a function of head radii. The frequency varies from above 80 kHz for mice ($a \cong 1$ cm) to about 8 kHz for humans ($a = 7$–10 cm).

We evaluate the constants A_m by using the initial conditions in (14) to obtain

$$A_m = -u_0 \left\{ \frac{a}{N\pi} \int_0^a r^2 j_1(k_m r) j_1\left(\frac{N\pi r}{a}\right) dr \pm \frac{4\mu}{3\lambda + 2\mu} \left(\frac{1}{N\pi}\right)^2 \int_0^a r^3 j_1(k_m r)\, dr \right\} \Bigg/ \left\{ \int_0^a r^2 [j_1(k_m r)]^2\, dr \right\}, \quad N = \begin{cases} 1,3,5,\cdots \\ 2,4,6,\cdots \end{cases} \tag{33}$$

The integrals in (33) may be evaluated [24] to give

$$\int_0^a r^2 j_1(k_m r) j_1\left(\frac{N\pi r}{a}\right) dr = \left[\frac{-a^3}{(k_m a)^2 - (N\pi)^2}\right]\left[\pm \frac{ka}{N\pi}\right] j_0(k_m a), \quad N = \begin{cases} 1,3,5,\cdots \\ 2,4,6,\cdots \end{cases} \tag{34}$$

$$\int_0^a r^3 j_1(k_m r)\, dr = \left(\frac{a^2}{k_m a}\right)^2 [3j_1(k_m a) - k_m a j_0(k_m a)] = \frac{a^3}{k_m} j_2(k_m a) \tag{35}$$

$$\int_0^a r^2 [j_1(k_m r)]^2\, dr = \frac{a^3}{2} \{[j_1(k_m a)]^2 - j_0(k_m a) j_2(k_m a)\} \tag{36}$$

where $j_2(k_m a)$ is the spherical Bessel function of the first kind and second order.

Using these values (33) becomes

$$A_m = \mp u_0 a \left(\frac{1}{N\pi}\right)^2 \left[\frac{2}{[j_1(k_m a)]^2 - j_0(k_m a) j_2(k_m a)}\right] \cdot \left\{ \frac{4\mu}{3\lambda + 2\mu} \left(\frac{1}{k_m a}\right) j_2(k_m a) - k_m a j_0(k_m a) \frac{1}{(k_m a)^2 - (N\pi)^2} \right\}, \quad N = \begin{cases} 1,3,5,\cdots \\ 2,4,6,\cdots \end{cases} \tag{37}$$

For $k_m a = m\pi = N\pi$, (37) simplifies to

$$A_m = -u_0 a \left(\frac{1}{N\pi}\right)\left[1 + \frac{24\mu}{3\lambda + 2\mu} \left(\frac{1}{N\pi}\right)^2\right]. \tag{38}$$

The displacement response of the sphere to a step input of microwave energy is now given by introducing (37) in (30) and then combining (24) and (30) in (15). We have

$$u(r,t) = u_0 Q + \sum_{m=1}^{\infty} A_m j_1(k_m r) \cos \omega_m t \tag{39}$$

$$Q = \frac{a}{N\pi} j_1\left(\frac{N\pi r}{a}\right) \pm \frac{4\mu}{3\lambda + 2\mu} \frac{r}{N^2\pi^2}, \quad N = \begin{cases} 1,3,5,\cdots \\ 2,4,6,\cdots \end{cases} \tag{40}$$

The radial stress can be deduced from the displacement solution using [22] and (13):

$$\sigma_r(r,t) = (\lambda + 2\mu) \frac{\partial u}{\partial r} + 2\lambda \frac{u}{r} - \beta v. \tag{41}$$

We have, therefore, by substituting (6), (10), and (39) into (41),

$$\sigma_r(r,t) = 4\mu u_0 S + \sum_{m=1}^{\infty} A_m k_m M_m \cos \omega_m t \tag{42}$$

$$S = \pm \left(\frac{1}{N\pi}\right)^2 - j_1\left(\frac{N\pi r}{a}\right) \Big/ \left(\frac{N\pi r}{a}\right), \quad N = \begin{cases} 1,3,5,\cdots \\ 2,4,6,\cdots \end{cases} \tag{43}$$

$$M_m = [(\lambda + 2\mu) j_0(k_m r) - 4\mu j_1(k_m r)/(k_m r)]. \tag{44}$$

2) Rectangular Pulse: We now can obtain the displacement and radial stress for a rectangular pulse of microwave energy by applying Duhamel's theorem [23] to the solutions expressed by (39) and (42). That is,

$$u(r,t) = \frac{\partial}{\partial t} \int_0^t F_t(t - t') u'(r,t')\, dt' \tag{45}$$

where $u'(r,t)$ is the solution given by (39) for the case of a sudden application of microwave radiation. An equivalent expression can, of course, be written for the radial stress. Therefore, by substituting (12) and (39) into (45), we have for the displacement

$$u(r,t) = u_0 Q t + \sum_{m=1}^{\infty} A_m j_1(k_m r) \frac{\sin \omega_m t}{\omega_m}, \quad 0 \le t \le t_0 \tag{46}$$

$$u(r,t) = u_0 Q t_0 + \sum_{m=1}^{\infty} A_m j_1(k_m r) \left[\frac{\sin \omega_m t}{\omega_m} - \frac{\sin \omega_m (t - t_0)}{\omega_m}\right], \quad t \ge t_0. \tag{47}$$

Similarly, we have for the radial stress

$$\sigma_r(r,t) = 4\mu u_0 St + \sum_{m=1}^{\infty} A_m k_m M_m \frac{\sin \omega_m t}{\omega_m}, \qquad 0 \le t \le t_0 \tag{48}$$

$$\sigma_r(r,t) = 4\mu u_0 St_0 + \sum_{m=1}^{\infty} A_m k_m M_m \cdot \left[\frac{\sin \omega_m t}{\omega_m} - \frac{\sin \omega_m (t - t_0)}{\omega_m}\right], \qquad t \ge t_0. \tag{49}$$

Equations (46)–(49) represent the general solution for the displacement and radial stress in a spherical head exposed to pulsed microwave radiation as a function of the microwave, thermal, elastic, and geometric parameters of the model.

Since u_0 and A_m are directly proportional to I_0, both the displacement and the radial stress are proportional to the peak absorbed power density. It is easy to see that the displacement and radial stress also depend linearly on the peak incident power density.

At the center of the sphere, $r = 0$, both (46) and (47) reduce to zero, and (48) and (49) become

$$\sigma_r = 4\mu u_0 \left[\pm \left(\frac{1}{N\pi}\right)^2 - \frac{1}{3}\right] t + \sum_{m=1}^{\infty} A_m k_m \left(\lambda + \frac{2}{3}\mu\right) \frac{\sin \omega_m t}{\omega_m}, \qquad 0 \le t \le t_0 \tag{50}$$

and

$$\sigma_r = 4\mu u_0 \left[\pm \left(\frac{1}{N\pi}\right)^2 - \frac{1}{3}\right] t_0 + \sum_{m=1}^{\infty} A_m k_m \left(\lambda + \frac{2}{3}\mu\right) \left[\frac{\sin \omega_m t}{\omega_m} - \frac{\sin \omega_m (t - t_0)}{\omega_m}\right], \qquad t \ge t_0, N = \begin{cases} 1,3,5,\cdots \\ 2,4,6,\cdots \end{cases} \tag{51}$$

The radial stress is therefore given by (50) and (51), and there is no displacement at the center of the model. On the other hand, at the surface ($r = a$), (43) becomes naught. The radial stress is given by the summation of the harmonic time functions alone.

III. Displacement and Sound Pressure

Using the parameters for brain matter given in Table I, we can compute the effect of microwave pulses on spherical models of the head from the solutions derived above. Fig. 5 shows the results of pressure computations in a 7-cm spherical head exposed to 918-MHz radiation with pulsewidth ranging from 0.1 to 100 μs while keeping the peak incident (or absorbed) power density constant. The relations between peak incident and absorbed power density are obtained from Figs. 2 and 3. The sound pressure amplitudes clearly depend on the pulsewidth of the impinging radiation. Moreover, there seems to be a minimum pulsewidth around 2 μs. The sound pressure amplitude rises rapidly first to a maximum and then alternates around a constant average amplitude. The dependence of sound pressure amplitude on peak powers is illustrated in Fig. 6. The pulsewidth is taken to be 20 μs. It is therefore apparent that the sound pressure amplitude depends upon peak power as well.

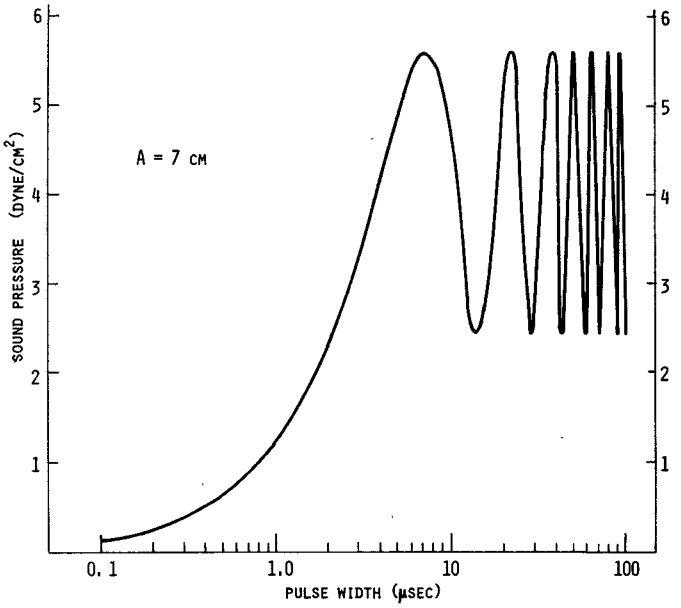

Fig. 5. Sound pressure amplitude generated in a 7-cm-radius spherical head exposed to 918-MHz plane wave as a function of pulsewidth. The peak absorbed energy is 1000 mW/cm³.

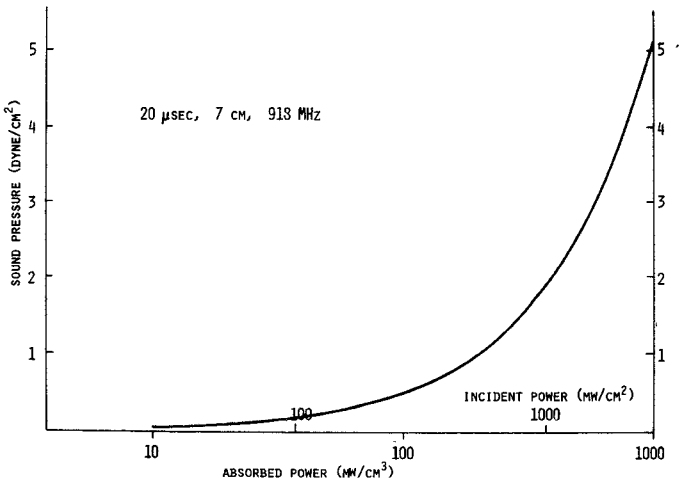

Fig. 6. The dependence sound pressure amplitude generated in a 7-cm-radius spherical head exposed to 918-MHz plane wave on peak incident and absorbed powers. The pulsewidth is taken to be 20 μs.

Fig. 7 gives the computed pressures in a 3-cm-radius sphere exposed to 2450-MHz radiation. It is readily seen that microwave-induced sound is a function of both pulsewidth and peak powers (Fig. 8). The minimum pulsewidth for efficient sound generation by 2450-MHz microwaves impinging on a 3-cm-radius spherical head is around 1 μs.

Figs. 9 and 10 depict typical displacements of brain matter in spherical models of the head exposed to pulsed microwaves. The pulsewidth used for computing Figs. 9 and 10 is 20 μs. These are representative graphs and are shown for $r = 0$, $a/2$, and a, where a is the radius of the sphere. As

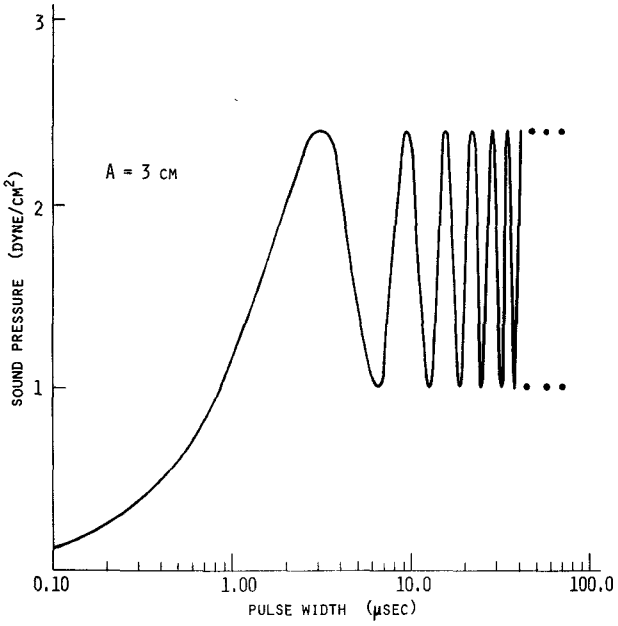

Fig. 7. Sound pressure amplitude generated in a 3-cm-radius spherical head exposed to 2450-MHz plane wave as a function of pulsewidth. The peak absorbed energy is 1000 mW/cm³.

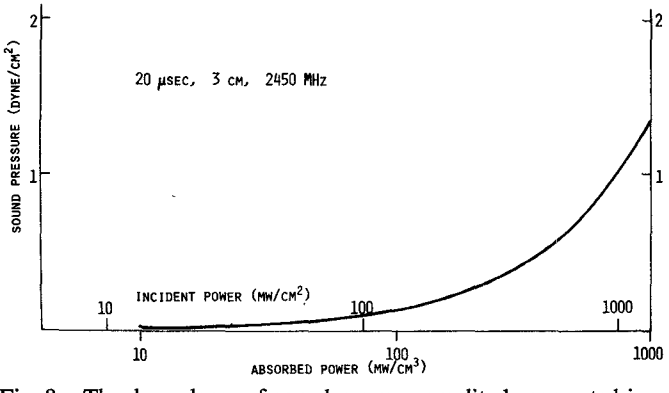

Fig. 8. The dependence of sound pressure amplitude generated in a 3-cm-radius spherical head exposed to 2450-MHz plane wave on peak incident and absorbed powers. The pulsewidth is taken to be 20 μs.

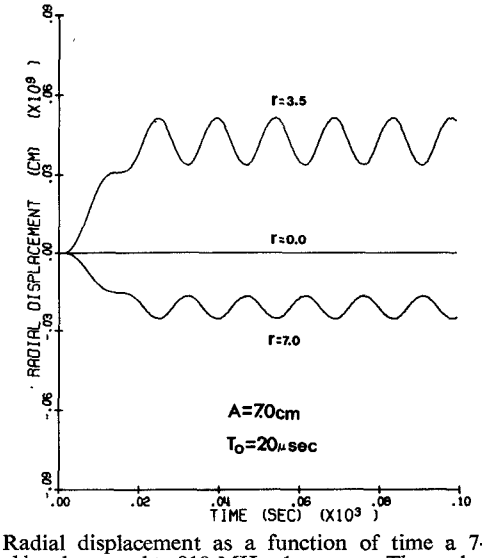

Fig. 9. Radial displacement as a function of time a 7-cm-radius spherical head exposed to 918-MHz plane wave. The peak absorption is 1000 mW/cm³.

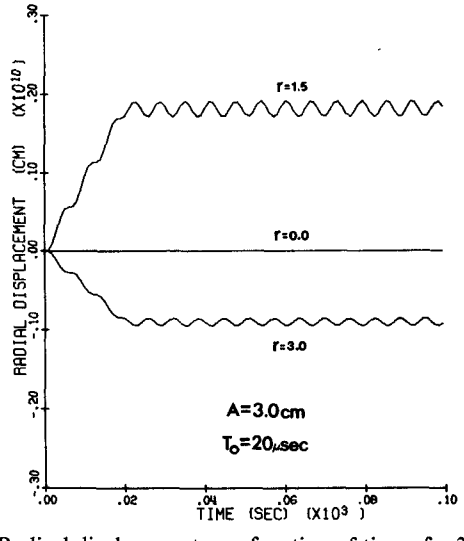

Fig. 10. Radical displacement as a function of time of a 3-cm-radius spherical head exposed to 2450-MHz plane wave. The peak absorption is 1000 mW/cm³.

expected, the displacement at the center of the sphere is zero. At other locations the displacement increases almost linearly as a function of time until $t = t_0$, the pulsewidth, and then starts to oscillate around the value attained at $t = t_0$. In both cases, the maximum displacements are on the order of 10^{-11} cm. The displacements stay constant after a transient buildup because of the lossless assumption for the elastic media. The apparent higher frequency of oscillation seems to stem from the contribution of higher order modes. But how these frequencies are chosen over all others is not clear. Further investigations are currently in progress.

The sound pressures (radial stresses) in the spherical head models are shown in Figs. 11 and 12 for the corresponding cases shown in Figs. 9 and 10. It is interesting to note that the sound pressure begins with zero amplitude and then grows to an intermediate value. With a sudden rise of amplitude the main body of the pressure wave arrives, oscillating at a constant pressure level in the absence of elastic loss. The final jump in amplitude is marked by $t = t_0$.

IV. Conclusions

We have presented a model for sound wave generation in spheres simulating heads of laboratory animals and human beings by assuming a spherically symmetric microwave absorption pattern. The impinging microwaves are taken to be plane wave rectangular pulses. The problem has been formulated in terms of thermoelastic theory in which the absorbed microwave energy represents the volume heat source. The thermoelastic equation of motion is solved for the sound wave under stress-free boundary conditions using boundary value technique and Duhamel's theorem. The extension to constrained surface is currently under investigation. It may be noted that the related case of micro-

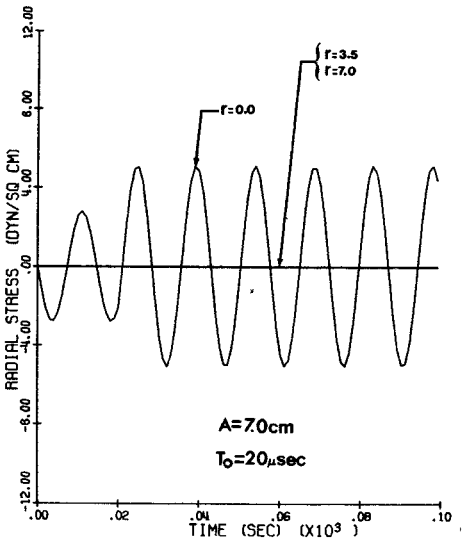

Fig. 11. Radial stress (sound pressure) generated in a 7-cm-radius spherical head exposed to 918-MHz plane wave. The peak absorption is 1000 mW/cm^3.

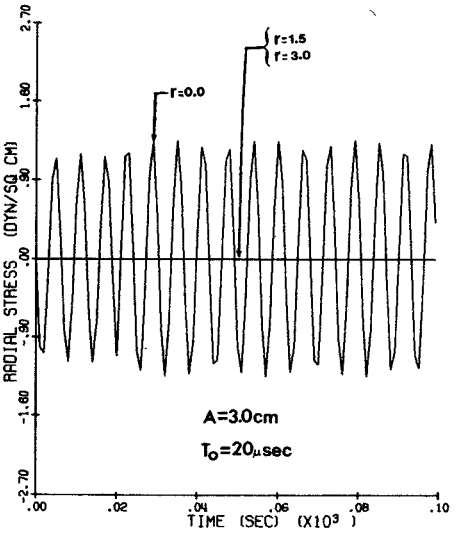

Fig. 12. Radial stress (sound pressure) generated in a 3-cm-radius spherical head exposed to 2450-MHz plane wave. The peak absorption is 1000 mW/cm^3.

wave pulses impinging on a semi-infinite medium of absorbing material has been given previously [25], [26].

Examination of the numerical results given in the last section indicates that pulsed microwave-induced sound pressure amplitude depends upon both pulsewidth and peak power density. In addition, there is apparently an optimal pulsewidth for maximum sound pressure generation which varies according to the sphere size and the frequency of the impinging radiation. As shown in Tables II and III, for a peak absorbed power density of 1000 mW/cm^3 (which corresponds to 600 mW/cm^2 incident power at 2450 MHz impinging on a 3-cm spherical head, and to 2200 mW/cm^2 incident power at 918 MHz impinging on a 7-cm spherical head), the pressure amplitudes generated at the center of the sphere are 15–30 dB above the reported threshold of hearing by bone conduction (60 dB, Re 0.0002 dyne/cm^2,

TABLE II
SOUND PRESSURE IN A MAN-SIZED (a = 7 cm) SPHERICAL HEAD EXPOSED TO 918-MHz RADIATION

Pulse width (μs)	Incident power mW/cm^2	Absorbed power mW/cm^3	Pressure (dyne/cm^2)	db re 0.0002 dyne/cm^2
0.1	2200	1000	0.12	55.5
0.5	2200	1000	0.60	69.5
1.0	2200	1000	1.19	75.5
5.0	2200	1000	4.90	87.8
10.0	2200	1000	4.70	87.4
20.0	2200	1000	5.10	88.1
30.0	2200	1000	2.80	82.9
40.0	2200	1000	4.10	86.2
50.0	2200	1000	5.40	88.6

TABLE III
SOUND PRESSURE IN A CAT-SIZED (a = 3 cm) SPHERICAL HEAD EXPOSED TO 2450-MHz RADIATION

Pulse width (μs)	Incident power (mW/cm^2)	Absorbed power (mW/cm^3)	Pressure (dyne/cm^2)	db re 0.0002 dyne/cm^2
0.1	600	1000	0.12	55.6
0.5	600	1000	0.59	69.4
1.0	600	1000	1.15	75.2
5.0	600	1000	1.40	76.9
10.0	600	1000	2.30	81.2
20.0	600	1000	1.35	76.6
30.0	600	1000	1.50	77.5
40.0	600	1000	2.2	80.8
50.0	600	1000	1.2	75.6

5–10 kHz) [27], [28] for pulses between 1 and 50 μs wide. The incident power required compares favorably with that reported previously [2], [4], [5]. At an absorbed power density of 1000 mW/cm^3, the corresponding rate of temperature rise at the center of both spheres, r = 0, is 0.258°C/s in the absence of heat conduction. The temperature rise in 20 μs is 5.2 × 10^{-6}°C.

Estimations of the fundamental sound frequency generated inside the head show that the frequency varies from about 8 kHz for a man-sized sphere to approximately 80 kHz for a small animal's, such as a mouse's, head. Assuming an equivalent radius of 1.5 cm for the brain of a guinea pig, Fig. 4 indicates a fundamental sound frequency of 48 kHz, which is in reasonably good agreement with the 50-kHz cochlea microphonic oscillations recorded from the round window of guinea pigs [6], which also happens to be the only available data in the literature,

Finally, it should be mentioned that the numerical results presented in this paper should be interpreted as giving estimates of the sound waves expected to be produced in mammalian heads by microwave pulses, subject to our ability to describe microwave, thermal, elastic, and geometric properties of mammalian cranial structures. In general, the results of this analysis indicate that thermoelastically generated stresses, resulting from microwave absorptive heating inside the head, represent a highly possible mechanism for sound generation.

ACKNOWLEDGMENT

The author wishes to thank P. M. Nefcy and C. K. Lam for their assistance.

REFERENCES

[1] A. H. Frey, "Auditory system response to radio frequency energy," *Aerospace Medicine*, vol. 32, pp. 1140–1142, 1961.
[2] A. W. Guy, E. M. Taylor, B. Ashleman, and J. C. Lin, "Microwave interaction with the auditory systems of humans and cats," *IEEE/MTT Symposium Digest*, pp. 321–323, 1973.
[3] E. M. Taylor and B. T. Ashleman, "Analysis of the central nervous involvement in the microwave auditory effect," *Brain Research*, vol. 74, pp. 201–208, 1974.
[4] A. W. Guy, C. K. Chou, J. C. Lin, and D. Christensen, "Microwave induced acoustic effects in mammalian auditory systems and physical materials," *Annals N.Y. Acad. Sciences*, vol. 247, pp. 194–215, 1975.
[5] W. J. Rissman and C. A. Cain, "Microwave hearing in mammals," *Proc. Nat. Elect. Conf.*, vol. 30, pp. 239–244, 1975.
[6] C. K. Chou, R. Galambos, A. W. Guy, and R. H. Lovely, "Cochlea microphonics generated by microwave pulses," *J. Microwave Power*, vol. 10, pp. 361–367, 1975.
[7] A. H. Frey, "Human auditory system response to modulated electromagnetic energy," *J. Appl. Physiol.*, vol. 17, pp. 689–692, 1962.
[8] A. H. Frey and R. Messenger, Jr., "Human perception of illumination with pulsed ultra-high frequency electromagnetic energy," *Science*, vol. 181, pp. 356–358, 1973.
[9] ANSI Standard, "Safety level of electromagnetic radiation with respect to personnel," *ANSI C95.1*, 1974.
[10] H. C. Sommer and H. E. von Gierke, "Hearing sensations in electric field," *Aerospace Med.*, vol. 35, pp. 834–839, 1964.
[11] J. C. Sharp, H. M. Grove, and O. P. Gandhi, "Generation of acoustic signals by pulsed microwave energy," *IEEE Trans. Microwave Theory Tech.*, vol. 22, pp. 583–584, 1974.
[12] K. R. Foster and E. D. Finch, "Microwave hearing: evidence for thermoacoustical auditory stimulation by pulsed microwaves," *Science*, vol. 185, pp. 256–258, 1974.
[13] J. C. Lin, "Microwave auditory effect—A comparison of some possible transduction mechanisms," *J. Microwave Power*, vol. 11, pp. 77–81, 1976.
[14] T. E. Cooper and G. J. Trezek, "A probe technique for determining the thermal conductivity of tissue," *J. Heat Transfer* vol. 94, pp. 133–138, 1972.
[15] G. T. Fallenstein, V. D. Hulce, and J. W. Melvin, "Dynamic mechanical properties of human brain tissue," *J. Biomechanics*, vol. 2, pp. 217–226, 1969.
[16] Y. C. Lee and S. H. Advani, "Transient response of a sphere to torsional loading—A head injury model," *Mathematical Bioscience*, vol. 6, pp. 473–486, 1970.
[17] J. A. Stratton, *Electromagnetic Theory*. New York: McGraw-Hill, 1941.
[18] J. C. Lin, A. W. Guy, and C. C. Johnson, "Power deposition in a spherical model of man exposed to 1–20 MHz electromagnetic fields," *IEEE Trans. Microwave Theory Tech.*, vol. 21, pp. 791–797, 1973.
[19] C. C. Johnson and A. W. Guy, "Nonionizing electromagnetic wave effects in biological materials and systems," *Proc. IEEE*, vol. 60, pp. 692–718, 1972.
[20] J. C. Lin, A. W. Guy, and G. H. Kraft, "Microwave selective brain heating," *J. Microwave Power*, vol. 8, pp. 275–286, 1973.
[21] H. S. Carslaw and J. C. Jaeger, *Conduction of heat in solids*, 2nd Edition. London: Oxford Univ. Press, 1959.
[22] A. E. H. Love, *A treaty on the mathematical theory of elasticity*. Cambridge, England, 1927.
[23] R. V. Churchill, *Operational mathematics*, 2nd edition. New York: McGraw-Hill, 1958.
[24] E. Jahnke and F. Emde, *Tables of functions*, 4th edition. New York: Dover, 1945.
[25] R. M. White, "Generation of elastic waves by transient surface heating," *J. Appl. Phys.*, vol. 34, pp. 3559–3569, 1963.
[26] L. S. Gournay, "Conversion of electromagnetic to acoustic energy by surface heating," *J. Acoust. Soc. Am.*, vol. 40, pp. 1322–1330, 1966.
[27] J. Zwislocki, "In search of the bone-conduction threshold in a free sound field," *J. Acous. Soc. Amer.*, vol. 29, pp. 795–804, 1957.
[28] J. F. Corso, "Bone-conduction thresholds for sonic and ultrasonic frequencies," *J. Acous. Soc. Amer.*, vol. 35, pp. 1738–1743, 1963.

Rank Reduction of Ill-Conditioned Matrices in Waveguide Junction Problems

DOUGLAS N. ZUCKERMAN, MEMBER, IEEE, AND PAUL DIAMENT, MEMBER, IEEE

Abstract—**A new low-rank spectral expansion technique for solving the ordinarily intractable matrix equations obtained from waveguide field equivalence theorem decompositions is described. The method facilitates the analysis of waveguide discontinuity problems that resist ordinary methods of solution. The technique is illustrated for the problem of scattering at a slant interface in a rectangular waveguide.**

I. INTRODUCTION

THE integral equations, and the corresponding matrix equations, that represent scattering at a waveguide discontinuity often exhibit ill-conditioned behavior. This results in computational difficulties as inversion of such matrices is inaccurate for even large-order truncated versions of the matrix. It is shown here, however, that it may be possible to take advantage of the often relatively low effective rank of the ill-conditioned portion of the matrix to overcome such difficulties.

In the following, a typical problem, that of scattering at a waveguide discontinuity, is solved by developing equations that are exact but ill conditioned. First, field equivalence theorems are used to reduce the structure to two uniformly filled waveguides with equivalent electric and magnetic current sheets at the discontinuity surface. Integral equations for the current sheets are then derived, using the null field condition in the two simpler waveguide structures. By writing series expansions for the current sheets, the integral equations are reduced to a system of linear algebraic equations for the current expansion coefficients. These exact equations are asymptotically ill conditioned. By a low rank spectral decomposition of the matrix representing the ill-conditioned portion of the equations, it is possible to solve for the currents without

Manuscript received June 14, 1976; revised February 4, 1977.
D. N. Zuckerman is with Bell Laboratories, Holmdel, NJ 07733.
P. Diament is with the Department of Electrical Engineering and Computer Science, Columbia University, New York, NY 10027.